Sādhanā (2020)45:261
https://doi.org/10.1007/s12046-020-01495-y

A compact printed ultra-wideband filtenna with low dispersion for WiMAX and WLAN interference cancellation

SURAJIT KUNDU

Department of ECE, National Institute of Technology Sikkim, Ravangla, South Sikkim 737139, India
e-mail: surajit.kundu@nitsikkim.ac.in

MS received 17 May 2020; revised 19 August 2020; accepted 24 August 2020

Abstract. A printed monopole filtenna fed by a co-planar waveguide with U-shaped split slot on patch and circular split ring resonator pairs at the other side of feed is proposed in this letter. The compact filtenna of dimension $0.32\lambda \times 0.215\lambda$ (λ denotes wavelength corresponding to 2.68 GHz) is capable of providing large bandwidth from 2.68 to 8.72 GHz with dual frequency notch bands over 3.28–3.84 and 4.95–6.02 GHz, primarily to eliminate the WiMAX and WLAN interferences. The dual notched antenna performances are evaluated by simulation and experimental measurement and compared to those of recently reported ultra-wideband (UWB) notched antennas. The proposed filtenna provides bidirectional E-plane and omni-directional H-plane radiation patterns with gain variation of 2–4.5 dBi and average radiation efficiency of 78% in its pass band. Also the filtenna offers minimal dispersion characteristic as stable group delay response, and linear variation of transfer function (S_{21}) is achieved in its pass bandwidth.

Keywords. Ultra-wideband (UWB) filtenna; frequency notch; printed monopole; circular split ring resonator (CSRR); U-slot.

1. Introduction

Ultra-wideband (UWB) communication is very promising in present wireless communication scenario as it delivers high throughput with very low transmitting power, which makes it suitable for multiple short-range communication applications such as ranging and localization, high-speed data link, wireless sensor network, body area network, UWB radar and bio-medical imaging [1]. One design constraint of all such UWB applications is the elimination of interferences from collocated wireless bands, which can be achieved by integrating desired band notch filter to the UWB antenna. However, addition of filter makes overall package bulky and complex with excess delay, higher power requirement and additional link budget. The implementation of notch characteristic in the antenna impedance band can solve the purpose without affecting the package size, system complexity and power requirement. Such notched antennas are also called filtennas, where filtering features are integrated. Various notch realization methods have been proposed in earlier literatures [2–18]. The simplest way of frequency notch creation is etching out slot in the radiator. Various slot shapes such as V [2], T [3], L [4] and H [5] were proposed earlier. However, such methods are prominent to produce a single notch. Also creation of multiple notches using slots is not suitable as it deteriorates antenna gain, radiation efficiency and pattern [6]. Frequency notches can also be realized by embedding stub [7], strip [8] and different resonating structures in the antenna geometry. However, these methods can generate a single notch only when applied individually. Therefore, combinations of two or more different notch generation techniques are adopted to realize multiple frequency stop bands in filtennas [9–17].

Da Xu *et al* [9] reported a UWB antenna of size 56×45 mm^2 that gave impedance band from 3 to 12 GHz with dual notches centred at 3.5 and 4.8 GHz. J. Y. Siddiqui *et al* [10] proposed a UWB circular monopole antenna with dual notches at 5.3–5.7 and 7.9–8.2 GHz. Jeon *et al* [11] used parallel strips for notch generation in an Archimedean spiral antenna to cover impedance band of 3.1–10.5 GHz, with 5.15–5.95 GHz notch band. A UWB antenna of size 80×70 mm^2 was reported in [12] that provided pass bandwidth of 1.5–12 GHz with four notches at 2.15–2.65, 3–3.7, 5.45–5.98 and 8–8.68 GHz. A balloon-shaped UWB antenna of dimension 27.5×16.5 mm^2 was reported in [13], which offered pass band from 1.75 to 10.3 GHz with two stop bands at 2.2–3.9 and 5.1–6 GHz. Peddakrishna and Khan [14] reported a UWB antenna that provided wide bandwidth of 2.7–11.7 GHz with two notches at 3.3–3.7 and 6.5–7.2 GHz. Siddiqui *et al* [15] reported a bulky antipodal tapered slot UWB antenna to realize multiple frequency notches. A CPW-fed UWB antenna of dimension 20×23 mm^2 was provided in [16] to realize dual stop bands at 4–5.78 and 6.83–8.22 GHz in

Published online: 17 October 2020

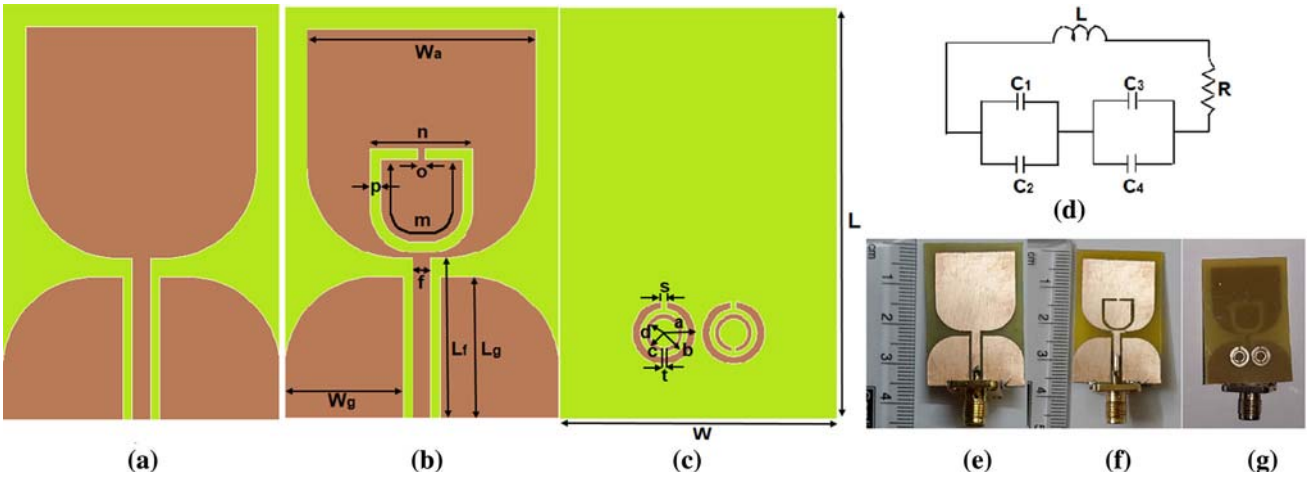

Figure 1. Schematic of (**a**) reference antenna, (**b**) top view and (**c**) bottom view of dual notched antenna, (**d**) equivalent circuit of circular split ring resonator, fabricated prototype of (**e**) reference antenna and (**f**) top view and (**g**) bottom view of filtenna.

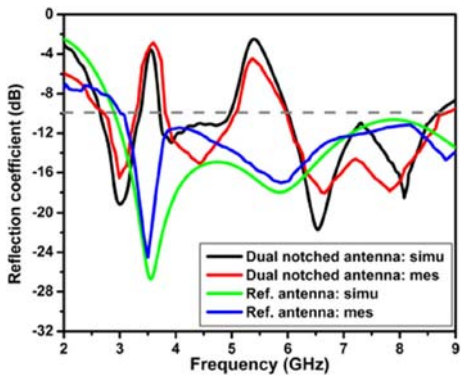

Figure 2. Comparison of simulated and measured reflection coefficients.

the impedance band from 3.2 to 10.5 GHz. Taher *et al* [17] reported a UWB antenna that gives frequency notch of 3.38–3.85 GHz in the 3.5–18 GHz impedance band. Gorai and Ghatak [18] reported a very compact dual notched UWB antenna with additional Bluetooth band where notches are realized at 5.5 and 8.1 GHz. One or more limitations such as bulky profile, improperly tuned frequency notch realization, poor *Q*-factor, reduced antenna gain and low radiation efficiency can be observed in the aforementioned UWB notched antennas.

UWB antennas are preferred to develop for various present and futuristic purposes such as 'frequency notched UWB antenna,' 'reconfigurable UWB antenna,' 'UWB antenna for cognitive radio' and 'UWB MIMO antenna' [1]. However one desired characteristic of all such UWB antennas is minimum dispersion, which ensures constant gain and pattern over frequency [19]. Linear phase response and flat group delay (*GD*) variation are desired over frequency of operation as they give fixed delay for all the frequency components and thus negligible dispersion [1].

A new dual notched U-shaped compact UWB filtenna with minimal dispersion is reported in this letter. The antenna geometry and notch realization structures are explained in the next section. The notched antenna performance is evaluated by simulation and experimental measurement in section 3 and finally the presented work is compared to recently reported multi-notched antennas in the conclusion section.

2. Design of antenna and notch structures

A U-shaped radiating patch, modified from the microstrip square patch antenna, is presented in [20]. Geometry of the reference antenna is presented in figure 1(a). Cone shapes are realized by producing flare angles between the bended peripheral of ground plane and lower peripheral of U-shaped patch at both sides of co-planar waveguide (CPW) feed. This configuration realizes additional higher resonance modes, to improve impedance bandwidth. Following equations are considered to evaluate antenna design parameters.

Total length (L) and width (W) of antenna can be calculated using equations (1)–(2):

$$0.3\lambda_L < L < 0.5\lambda_L, \tag{1}$$

$$W \approx 0.25\lambda_L. \tag{2}$$

Width (W_a) of square-shaped bended patch is obtained from

$$W_a \approx 0.2\lambda_L. \tag{3}$$

Dimensions (length L_g and width W_g) of co-planar antenna ground can be calculated from

$$L_g \approx 0.125\lambda_L, \tag{4}$$

Table 1. Comparison of theoretically computed, simulated and measured notch centre frequency (f_n) values.

Notch realization method	Theoretically computed f_n (GHz)	Simulated f_n (GHz)	Measured f_n (GHz)
Slot	3.5868	3.51	3.55
CSRR	5.49	5.4	5.42

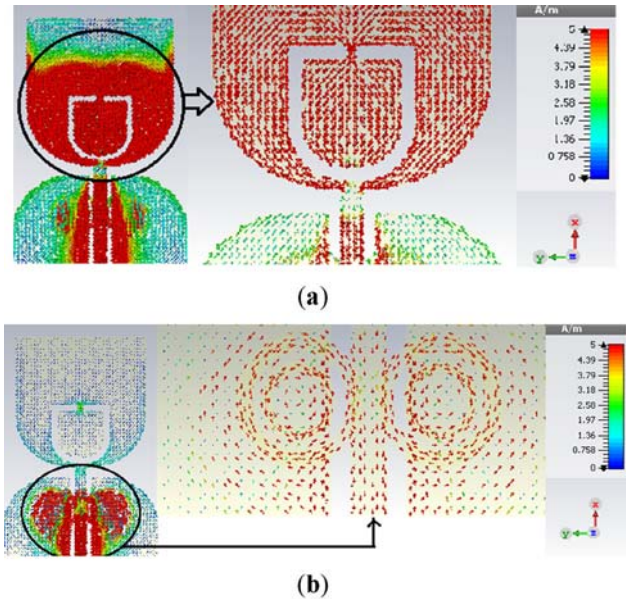

Figure 3. Simulated surface current of dual notched antenna at (**a**) 3.55 GHz and (**b**) 5.4 GHz.

$$0.11\lambda_L < W_g < 0.1\lambda_L. \tag{5}$$

In all these equations λ_L represents wavelength calculated from lower band-edge of UWB, which is 3.1 GHz. Frequency notch geometry is implemented to mitigate the antenna band operating from the collocated wireless bands.

As can be seen in figure 1(b), U-shaped patch like split ring resonator slot is embedded in the lower portion of antenna patch close to feed gap. Targeting the WiMAX band (3.3–3.8 GHz) notch centred at 3.55 GHz, the slot dimensions can be obtained from equation (6):

$$f_n = \frac{c}{[2(m+p)+o]\sqrt{\varepsilon_e}}. \tag{6}$$

Here c represents the speed of light and $\varepsilon_e = \frac{\varepsilon_r+1}{2}$ where ε_r represents relative permittivity of substrate, which is considered to be 4.4.

Two co-directional and symmetric circular split ring resonators (CSRRs) are placed side by side at the bottom of substrate, other end of CPW feed to realize WLAN band notch.

A schematic of antenna's back view with CSRR geometry is shown in figure 1(c). Operation of CSRR can be explained with the help of its equivalent circuit drawn in figure 1(d). The CSRR can be thought of as a parallel LC resonator where current is induced in the coupled circular metallic split rings due to electromotive force (EMF) that appears around the CSRR because of external excitement. Distributed capacitances (C_1 and C_3) are produced in the inner spacing of metallic rings at both halves of CSRR, and inductance (L) is produced when current passes from one circular split ring to another through the inner space. The gap capacitances (C_2 and C_4) are produced because of the split in the circular rings. The total capacitance and

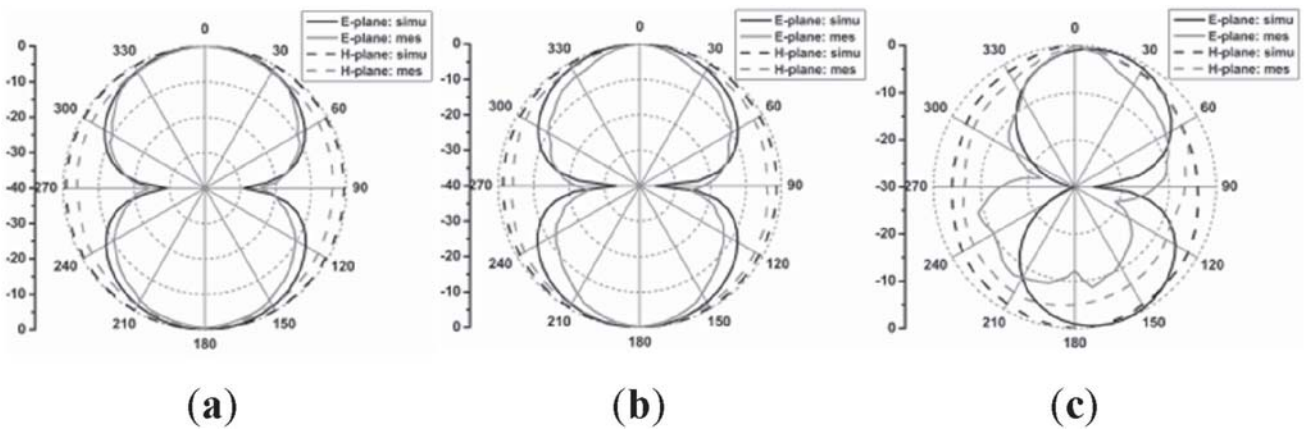

Figure 4. Simulated and measured co-polarized antenna radiation patterns at (**a**) 3 GHz, (**b**) 6.6 GHz and (**c**) 8 GHz.

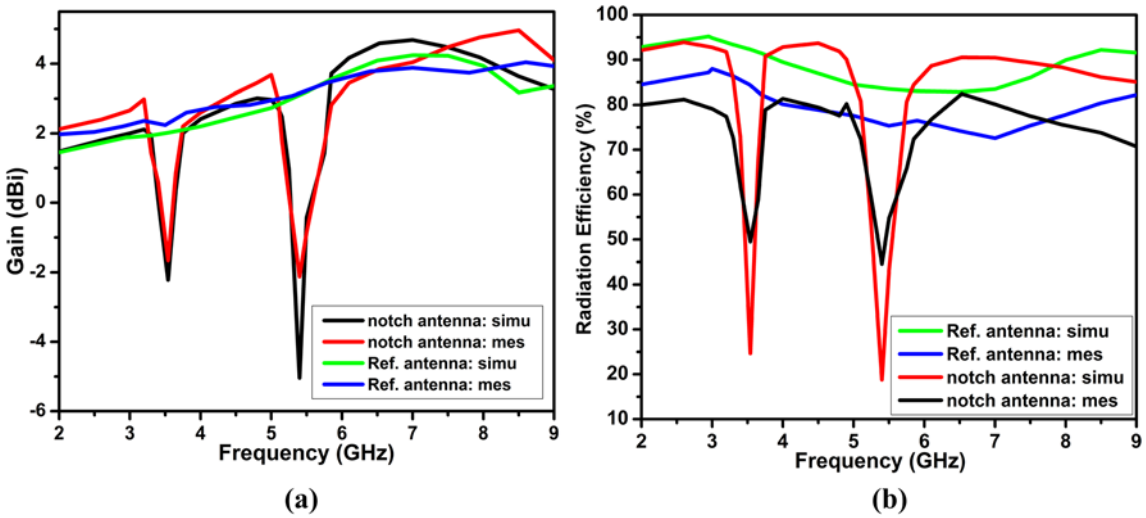

Figure 5. Simulated and measured (**a**) gain response and (**b**) radiation efficiency of reference and dual notched antennas.

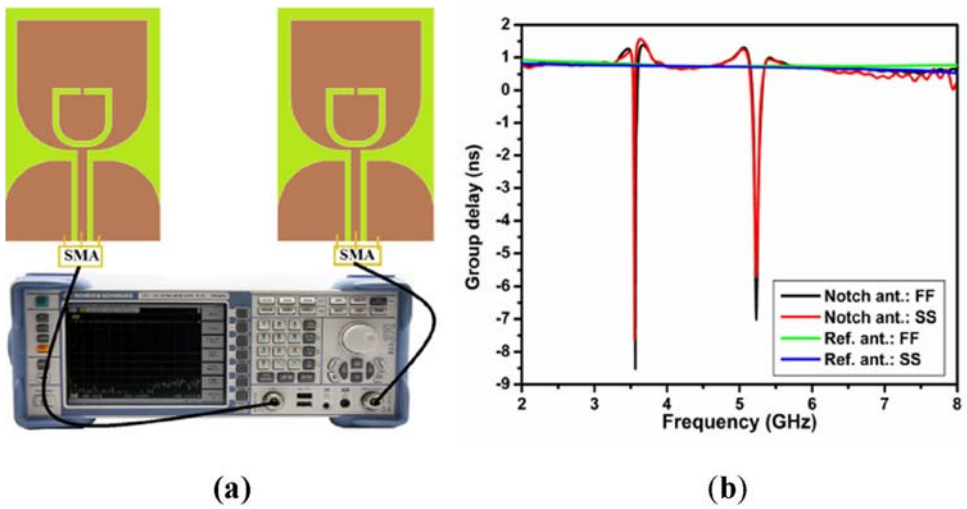

Figure 6. (**a**) Group delay and transfer function (S_{21}) measurement set-up in side–by-side orientation and (**b**) group delay comparison plots for reference antenna and proposed filtenna.

inductance are calculated using equations (7) and (8), respectively [21, 22]:

$$C = \frac{(C_1 + C_2)(C_3 + C_4)}{(C_1 + C_2) + (C_3 + C_4)} \tag{7}$$

$$L = \frac{a}{100 \times 25.4}\left[7.4 \log \frac{32a}{r} - 6.4\right] \mu\text{H} \tag{8}$$

$$\text{where } r = \frac{(a-b) + (c-d)}{2}. \tag{9}$$

The notch centre frequency can be evaluated using equation (10):

$$f_n = \frac{1}{2\pi\sqrt{LC}}. \tag{10}$$

The design parameters are optimized by parametric study using a CST microwave studio suite simulator [23]. The optimal values of design parameters are as follows: $L = 0.372\ \lambda_L$; $W = 0.248\ \lambda_L$; $W_a = 0.2\ \lambda_L$; $W_g = 0.107\ \lambda_L$; $L_f = 0.165\lambda_L$; $L_g = 0.1447\lambda_L$; $f = 0.016\lambda_L$; $m = 0.248\lambda_L$; $n = 0.1\lambda_L$; o = s $= 0.006\ \lambda_L$; $p = 0.0124\ \lambda_L$; $t = 0.004\ \lambda_L$; $a = 0.025\ \lambda_L$; $b = 0.02\lambda_L$; $c = 0.0165\lambda_L$ and $d = 0.013\lambda_L$. As shown in figure 1(e)–(g) the filtenna structure is fabricated on inexpensive and certainly available FR4 epoxy substrate, which has relative permittivity 4.4, loss tangent 0.02 and thickness 0.8 mm only. The calculated WiMAX notch centre frequency (f_n) value is 3.5868 GHz as obtained from equation (6), using the optimal values of design parameters. Also the total capacitance (C) and inductance (L) values are obtained as 0.086 pF and 9.78 nH,

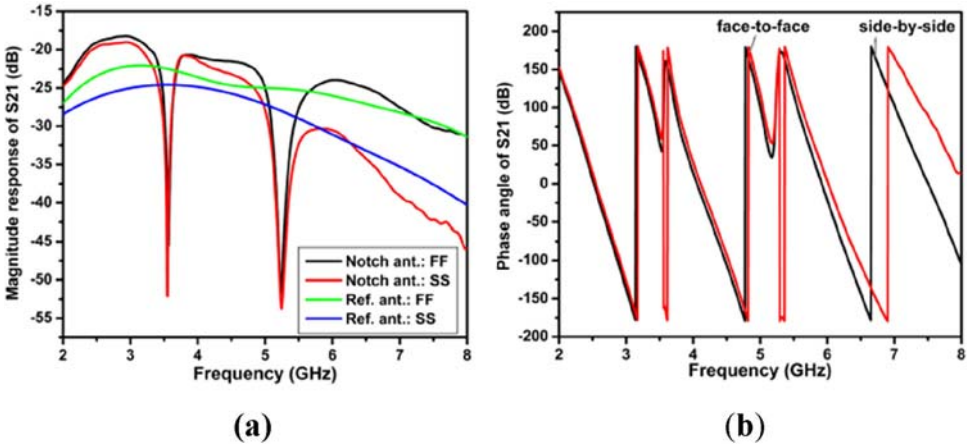

Figure 7. (**a**) Magnitude response of transfer function for reference antenna and filtenna. (**b**) Phase response of filtenna, in face-to-face and side-by-side orientations.

respectively, from equations (7)–(9). Finally, the notch centre frequency due to CSRR is obtained as 5.49 GHz from equation (10).

3. Results and discussion

The proposed filtenna and the reference antenna are simulated using the CST microwave studio suite and the simulated results are verified by experimental measurements. The simulated and measured impedance bandwidths ($S_{11} < -10$ dB) of the reference and proposed dual notched antennas are plotted in figure 2. The proposed filtenna offers measured bandwidth from 2.68 to 8.72 GHz with dual frequency stop bands at 3.28–3.84 and 4.95–6.02 GHz that has good similarity with the simulated plots. The simulated and measured notch centre frequency values are in good agreement with the theoretically computed notch centre values as shown in table 1.

Simulated surface currents of the proposed filtenna at notch centre frequencies, i.e. 3.55 and 5.4 GHz, are plotted in figure 3. Very condensed current distribution around the U-shaped split ring slot at 3.55 GHz can be seen. However the current flow is opposite directional inside and outside the slot, which effects cancellation to each other and results in strong frequency rejection. Similarly, at 5.4 GHz, strong surface current around the CSRR pair can be observed that has clockwise and counterclockwise current flow in the split rings to produce strong frequency cancellation.

Antenna radiation patterns at 3, 6.6 and 8 GHz are plotted in figure 4. Clearly the antenna exhibits bidirectional E-plane and omnidirectional H-plane patterns at all three frequencies, which are similar to the conventional monopole antenna patterns. Also, good matching between the simulated and measured radiation patterns can be observed.

Antenna gain variation over frequency can be observed in figure 5(a). The reference antenna exhibits gain variation from 1.5 to 4.5 dBi, and the proposed dual notched antenna offers flat gain variation of 2–4.5 dBi in its pass band with notable aberration in the dual stop bands. The significant suppression in the simulated and measured gain values of filtenna implies the realization of strong frequency rejection around the notch centre frequencies.

Radiation efficiency of such UWB antennas can be measured using rectangular aluminum boxes following the modified Wheeler's cap method as proposed in [24]. As plotted in figure 5(b), the reference antenna exhibits measured radiation efficiency variation of 75–87% in 2–9 GHz frequency band whereas the proposed filtenna offers radiation efficiency variation of 72–84% in its pass band as per measurement. A difference in radiation efficiency of about 10% can be observed between simulated and measured plots primarily due to the assumption of Wheeler's cap method. Also, a noteworthy eccentricity in radiation efficiency can be observed in the dual stop bands that authenticates strong notch creation.

The transient analysis of proposed filtena is conducted by examining its *GD*, transfer function (S_{21}) responses and comparing to *GD*, S_{21} responses of reference antenna. *GD* and S_{21} can be measured by keeping two similar test prototypes in face-to-face and side-by-side orientations and connecting the prototypes with a dual port vector network analyser as shown is figure 6(a). The *GD* responses are flat for the reference antenna and filtenna in both the orientations (figure 6(b)); however, sudden strong variations ($> \pm 1$ ns) in *GD* response can be seen in the notch bands of proposed filtenna that justify the notch creation. Similarly, it is evident from figure 7(a) that both the reference antenna and the filtenna offer linear variations in the magnitude response of transfer function (S_{21}) for both the orientations whereas sharp irregularities can be observed in the dual

Table 2. Comparison of proposed UWB filtenna with recently reported UWB notched antennas.

Ref./ Year	Size in mm^2	Notch generating method	No. of notches	Pass band (GHz)	Notch bands (GHz)	*Gain (dBi)	*Avg. rad. eff.	Remark
[9]/ 2014	56 × 45	SLRR slot	2	3–12	Centred at 3.5 and 4.8	1–6	80%	Improperly tuned notch
[10]/ 2015	50 × 50	Split ring resonator	2	2.5–11	5.3–5.7; 7.9–8.2	0–4	–	Improperly tuned notch
[11]/ 2016	36 × 36	Parallel strips	1	3.1–10.5	5.15–5.95	3-5	–	Only single notch band
[12]/ 2017	80 × 70	Systematic defection slots	4	1.5–12	2.15–2.65, 3–3.7, 5.45–5.98, 8–8.68	0-6	75%	Bulky profile, improperly tuned notches
[13]/ 2018	27.5 × 16.5	U-slot and parasitic resonator	2	1.75–10.3	2.2–3.9, 5.1–6	2-4.5	80%	Poor roll-off, loss of spectrum
[14]/ 2018	40 × 52	π-shaped slot and EBG resonator	2	2.7–11.7	3.3–3.7, 6.5–7.2	1-5	–	Improperly tuned notch
[15]/ 2018	307.4 × 282	SRR	Variable	0.4–9	2.55; 2.95; 3.2; 4.1	5–10	–	Bulky profile
[16]/ 2019	20 × 23	Circular split ring slots	2	3.2–10.5	4–5.78 and 6.83–8.22	0.5-4.83	95%	Improperly tuned notches
[17]/ 2019	20 × 20	C-shaped slot	1	3.5–18	3.38–3.85	–	–	Only single notch band
[18]/ 2019	14 × 32	Modified ELC resonator	2	2.4 and 3–12	Centred at 5.5 and 8.1	0–4	–	Improperly tuned notches
This work	36 × 24	U-shaped split slot and CSRR	2	2.68–8.72	3.28–3.84 4.95–6.02	2–4.5	78%	Compact, properly tuned dual notches

*Values are valid in pass band only.

notch bands of filtenna. The phase responses of filtenna's transfer function in side-by-side and face-to-face orientations are plotted in figure 7(b). Linear phase responses can be seen in the pass bandwidth of reference antenna and proposed filtenna, whereas extensive non-linearity can be seen at dual notch bands of filtenna. Flat *GD* and linear phase–frequency responses in the pass band of proposed filtenna ensure stationary phase centre and thus uniform transmission of all frequency components, which therefore guarantee the low dispersion characteristic. Notable non-linearity at dual notch bands ensures the strong frequency rejection.

4. Conclusion

A printed UWB monopole filtenna of size $36 \times 24 \times 0.8\ \text{mm}^3$ with WiMAX and WLAN notch cancellation is proposed in this letter. The proposed filtenna offers stable gain response, high radiation efficiency and non-directional patterns with stable GD and linear transfer function response in its pass bandwidth. The proposed filtenna can be used for short-range indoor communication, ad-hoc wireless application, impulse radar and microwave imaging applications. Measured results of the filtenna parameters are compared with some of the recently reported notched antennas in table 2. Clearly the proposed compact dual notched antenna is superior in terms of its performance for UWB applications.

References

[1] Saha C, Siddiqui J Y and Antar Y M M 2019 *Multifunctional Ultrawideband Antennas: Trends, Techniques and Applications*, 1st ed. USA: CRC Press

[2] Kim Y and Kwon D H 2004 CPW-fed planar ultra wideband antenna having a frequency band notch function. *Electron. Lett.* 40(7): 403–405

[3] Ojaroudi M, Ghobadi C and Nourinia J 2009 Small square monopole antenna with inverted T-shaped notch in the ground plane for UWB application. *IEEE Antennas Wirel. Propag. Lett.* 8: 728–731

[4] Farrokh-Heshmat N, Nourinia J and Ghobadi C 2009 Band-notched ultra-wideband printed open-slot antenna using variable on-ground slits. *Electron. Lett.* 45(21): 1060–1061

[5] Deng J Y, Yin Y Z, Zhou S G and Liu Q Z 2008 Compact ultra-wideband antenna with tri-band notched characteristic. *Electron. Lett.* 44(21): 1231–1233

[6] Ojaroudi N and Ojaroudi M 2013 Ultra-wideband slot antenna with a stop-band notch. *IET Microw. Antennas Propag.* 7(10): 831–835

[7] Cai L Y, Zeng G, Yang H C and Zhan X W 2010 Compact printed ultra-wideband antennas with band-notched characteristics. *Electron. Lett.* 46(12): 817–819

[8] Ghobadi A, Ghobadi C and Nourinia J 2010 A novel band-notched planar monopole antenna for ultrawideband applications. *IEEE Antennas Wirel. Propag. Lett.* 9: 608–611

[9] Da Xu K, Zhang Y H, Spiegel R J, Fan Y, Joines W T and Liu Q H 2014 Design of a stub-loaded ring-resonator slot for antenna applications. *IEEE Trans. Antennas Propag.* 63(2): 517–524

[10] Siddiqui J Y, Saha C and Antar Y M 2014 Compact dual-SRR-loaded UWB monopole antenna with dual frequency and wideband notch characteristics. *IEEE Antennas Wirel. Propag. Lett.* 14: 100–103

[11] Jeon J H, Chang J T and Pham A V 2016 Characterization, analysis, and implementation of integrated bandstop structures on ultra-wideband Archimedean spiral antenna. *IEEE Trans. Antennas Propag.* 64(5): 1999–2004

[12] ur Rehman S and Alkanhal M A 2017 Design and system characterization of ultra-wideband antennas with multiple band-rejection. *IEEE Access* 5: 17988–17996

[13] Kundu S 2018 Balloon-shaped CPW fed printed UWB antenna with dual frequency notch to eliminate WiMAX and WLAN interferences. *Microw. Opt. Technol. Lett.* 60(7): 1744–1750

[14] Peddakrishna S and Khan T 2018 Design of UWB monopole antenna with dual notched band characteristics by using π-shaped slot and EBG resonator. *AEU – Int. J. Electron. Commun.* 96: 107–112

[15] Siddiqui J Y, Saha C, Sarkar C, Shaik L A and Antar Y M M 2018 Ultra-wideband antipodal tapered slot antenna with integrated frequency-notch characteristics. *IEEE Trans. Antennas Propag.* 66(3): 1534–1539

[16] Awan W A, Zaidi A, Hussain N, Iqbal A and Baghdad A 2019 Stub loaded, low profile UWB antenna with independently controllable notch-bands. *Microw. Opt. Technol. Lett.* 61(11): 2447–2454

[17] Taher N, Elftouh H, Zakriti A and Touhami N A 2019 CPW-fed planar ultra-wideband notched antenna at WiMAX frequency. *Procedia Manuf.* 32: 723–728

[18] Gorai A and Ghatak R 2019 Multimode resonator-assisted dual band notch UWB antenna with additional bluetooth resonance characteristics. *IET Microw. Antennas Propag.* 13(11): 1854–1859

[19] Schantz H G 2015 *The Art and Science of Ultrawideband Antennas*, 2nd ed. USA: Artech House

[20] Pachigolla S Y and Kundu S 2018 A compact bandwidth enhanced monopole antenna for ultra-wideband applications. In: *Proceedings of the IEEE Indian Conference on Antennas and Propogation (InCAP)*, pp. 1–4

[21] Saha C and Siddiqui J Y 2011 A comparative analysis for split ring resonators of different geometrical shapes. In: *Proceedings of the 2011 IEEE Applied Electromagnetics Conference (AEMC)*, pp. 1–4

[22] Terman F E 1943 *Radio Engineers' Handbook*, 1st ed. New York and London: McGraw-Hill

[23] CST Microwave Studio 2016 Computer Simulation Technology (CST), Germany. Available at: https://www.cst.com/Products/CSTMWS

[24] Muramoto M, Ishii N and Itoh K 1996 Radiation efficiency measurement of a small antenna using the wheeler method. *Electron. Commun. Jpn. (Part I: Commun.)* 79(6): 93–100